Supplementary Information (SI) for Environmental Science: Atmospheres.
This journal is © The Royal Society of Chemistry 2025

Supplementary Materials

Two approaches to mass closure analysis for carbon-rich aerosol in Metro Manila, Philippines

Grace Betito[1,2,3*], Grethyl Catipay-Jamero[1,2,4], Honey Alas[5], Wolfram Birmili[5,6], Maria Obiminda Cambaliza[1,2], Mylene Cayetano[7], David Cohen[8], Melliza Cruz[2], Maria Cecilia Galvez[9], Arvin Jagonoy[10], Simonas Kecorius[11,12], Genevieve Rose Lorenzo[2], Leizel Madueño[5], Thomas Müller[5], Preciosa Corazon Pabroa[10], James Bernard Simpas[1,2], Armin Sorooshian[3,13], Everlyn Gayle Tamayo[7], Edgar Vallar[9], Kay Weinhold[5], and Alfred Wiedensohler[5]

[1]Department of Physics, Ateneo de Manila University, Katipunan Ave., Quezon City, Philippines
[2]Manila Observatory, Ateneo de Manila Campus, Quezon City, Philippines
[3]Department of Hydrology and Atmospheric Sciences, University of Arizona, Tucson, AZ, USA
[4]Caraga State University-Cabadbaran Campus, Cabadbaran City, Agusan del Norte, Philippines
[5]Leibniz Institute for Tropospheric Research, Leipzig, Germany
[6]German Environment Agency (Umweltbundesamt), Berlin, Germany
[7]Institute of Environmental Science and Meteorology, University of the Philippines Diliman, Philippines
[8]Australian Nuclear Science and Technology Organization, Menai, Australia
[9]Environment And Remote Sensing Research (EARTH) Laboratory, Department of Physics, De La Salle University, Manila, Philippines
[10]Philippine Nuclear Research Institute - Department of Science and Technology, Quezon City, Philippines
[11]Institute of Epidemiology, Helmholtz Zentrum München - German Research Center for Environmental Health, Neuherberg, Germany
[12]Environmental Science Center, University of Augsburg, Augsburg, Germany
[13]Department of Chemical and Environmental Engineering, University of Arizona, Tucson, AZ, USA

Equation S1: Error estimation for gravimetric mass

We used error propagation equation (Eq. S1)[1] to estimate the overall uncertainty of the gravimetric mass as a combination of uncertainties in weighing, as well as sampling air volume.

$$SD_d = \sqrt{SD_b^2 + SD_a^2} \quad \text{Eq. (S1)}$$

where SD_d is the standard deviation of the difference, SD_b is the standard deviation of the substrate weight/sampling air volume before sampling, and SD_a is the standard deviation of the substrate weight/sampling air volume after sampling.

Equation S2: Error estimation for elemental mass

"For the analysis of elemental components, total error estimates were calculated by adding individual error estimates in quadrature, as shown in Equation (S1), including at least three components: measurement calibration errors (Calib), experimental measurement errors (Expt), and statistical counting errors (Stats).[2]"

$$Error^2 = Calib^2 + Expt^2 + Stats^2 + \ldots \quad \text{Eq. (S2)}$$

Table S1. Modified IMPROVE_A protocol used for OC-EC analysis

Protocols	IMPROVE-A	IMPROVE-A edit
Step	T (°C)	T (°C)
OC1	140	140
OC2	280	280
OC3	480	480
OC4	580	650
EC1	580	580
EC2	740	740
EC3	840	840

Table S2. Summary of chemical analyses performed on Teflon and quartz filters, including the corresponding instruments and the year each analysis was completed.

Chemical Analysis	Instrument	Year Completed
Teflon Filters		
a) Elemental species	PIXE	2015
b) Water-soluble ions	IC	2017
Quartz Filters		
a) OC and EC	OC-EC Analyzer	2015

Table S3. Pearson's correlation matrices (r values) between water-soluble ions, carbonaceous components, and elemental species for A) KAT RS, B) MO UB, and C) TAFT RS during the MACE 2015 campaign. Blank cells represent statistically insignificant values.

A.)															
OC	1.00														
EC		1.00													
NH_4	0.66		1.00												
K	0.32			1.00											
Mg				0.77	1.00										
Cl				0.65	0.84	1.00									
NO_3	0.38			0.52	0.46	0.66	1.00								
SO_4	0.70		0.90	0.37			0.38	1.00							
Al				0.80	0.77	0.81	0.30		1.00						
Si	0.44			0.68	0.68	0.64	0.60	0.54	0.83	1.00					
Ca		0.50		0.52	0.54	0.56	0.43	0.42	0.68	0.85	1.00				
Mn		0.51	0.65					0.49				1.00			
Fe	0.32	0.59		0.34			0.38	0.53		0.70	0.82	0.47	1.00		
Cu				0.70	0.68	0.61	0.34		0.75	0.61	0.62		0.31	1.00	
Zn										0.37	0.31	0.37	0.57	0.55	1.00
	OC	**EC**	**NH_4**	**K**	**Mg**	**Cl**	**NO_3**	**SO_4**	**Al**	**Si**	**Ca**	**Mn**	**Fe**	**Cu**	**Zn**

B.)													
OC	1.00												
EC		1.00											
NH_4	0.75		1.00										
K	0.83	0.36	0.57	1.00									
Mg		0.30	0.32	0.36	1.00								
Cl					0.45	1.00							
NO_3		0.78	0.31	0.56	0.85		1.00						
SO_4	0.76	0.31	0.96	0.61			0.42	1.00					
Si	0.70		0.67	0.60				0.49	1.00				
Ca	0.33		0.64	0.37	0.37	0.42			0.37	1.00			
Mn		0.59	1.00		0.86	1.00	0.78			0.95	1.00		
Fe	0.34		0.66	0.39	0.55	0.49			0.36	0.97	0.94	1.00	
Zn	0.43		0.65	0.53	0.53		0.30		0.30	0.94	0.96	0.96	1.00
	OC	**EC**	**NH_4**	**K**	**Mg**	**Cl**	**NO_3**	**SO_4**	**Si**	**Ca**	**Mn**	**Fe**	**Zn**

C.)													
OC	1.00												
EC	0.84	1.00											
NH_4		0.60	1.00										
K	0.64	0.38		1.00									
Mg	0.38	0.43	0.37		1.00								
NO_3	0.58	0.58	0.58			1.00							
SO_4	0.33	0.59	0.96		0.34	0.51	1.00						
Al								1.00					
Si	0.30			0.46				0.60	1.00				
Ca	0.45			0.44		0.40		0.79	0.45	1.00			
Mn								0.99	0.73	0.62	1.00		
Fe	0.67	0.41		0.67				0.39	0.53	0.79	0.39	1.00	
Zn	0.52			0.68				0.40	0.61	0.82	0.48	0.88	1.00
	OC	**EC**	**NH_4**	**K**	**Mg**	**NO_3**	**SO_4**	**Al**	**Si**	**Ca**	**Mn**	**Fe**	**Zn**

Table S4. Two-mode lognormal model parameters for number-derived mass size distribution. *C*: mass concentration; D_g: geometric mean diameter; σ_g: geometric standard deviation.

(a) Mass size distribution	C_1 (µg m^{-3})	$D_{g,1}$ (nm)	$\sigma_{g,1}$	C_2 (µg m^{-3})	$D_{g,2}$ (nm)	$\sigma_{g,2}$
KAT RS	76.5	209	2.09	64.2	2964	1.72
MO UB	48.3	234	1.97	44.4	2790	1.64
TAFT RS	73.9	185	2.08	65.3	3381	1.84

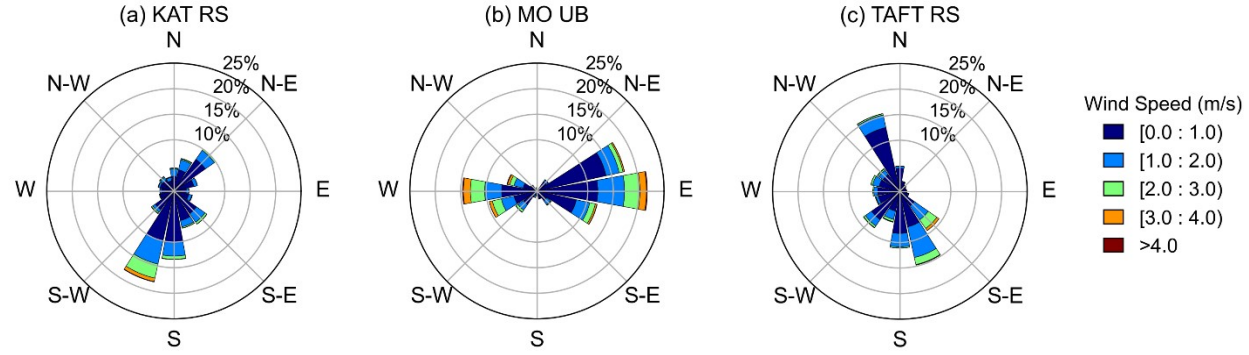

Figure S1. Wind rose plot for (a) KAT RS, (b) MO UB, and (c) TAFT RS averaged for the duration of the sampling.

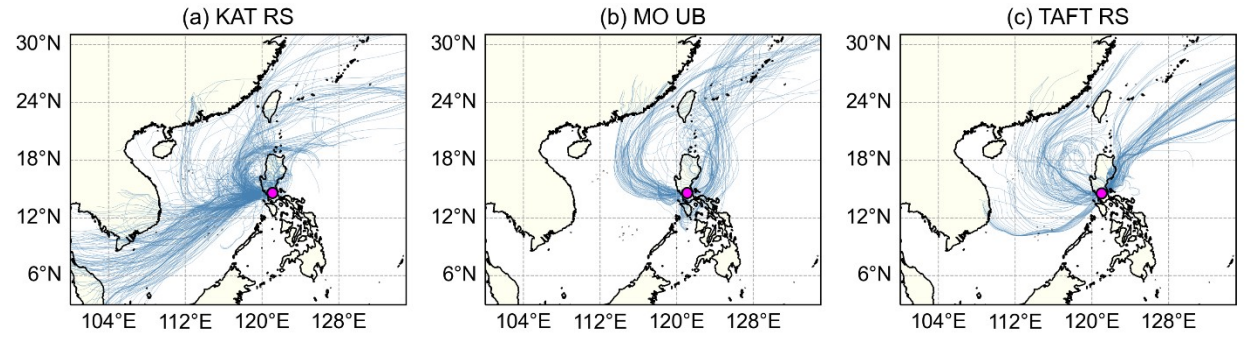

Figure S2: HYSPLIT back trajectories for (a) KAT RS, (b) MO UB and (c) TAFT RS, with those locations denoted by the pink circles in each respective panel. Results shown are based on five-day back trajectories generated every hour using GDAS data at 500 m above ground level.

Reference

1. C. Stahl, M. T. Cruz, P. A. Banaga, G. Betito, R. A. Braun, M. A. Aghdam, M. O. Cambaliza, G. R. Lorenzo, A. B. MacDonald, P. C. Pabroa, J. R. Yee, J. B. Simpas and A. Sorooshian, An annual time series of weekly size-resolved aerosol properties in the megacity of Metro Manila, Philippines, *Sci Data*, 2020, **7**, 128.
2. D. D. Cohen, The IAEA/ RCA fine and coarse particle ambient air database. Lucas Heights, NSW: Australian Nuclear Science and Technology Organisation. http://apo.ansto.gov.au/dspace/handle/10238/6404.*Journal*, 2010.